

ROTATION CURVES FROM BARYONIC INFALL: DEPENDENCE ON DISK-TO-HALO RATIO, INITIAL ANGULAR MOMENTUM, AND CORE RADIUS, AND COMPARISON WITH DATA¹

RICARDO FLORES

Department of Physics and Astronomy, University of Missouri, Saint Louis, MO 63121

JOEL R. PRIMACK

Santa Cruz Institute for Particle Physics, University of California, Santa Cruz, CA 95064

GEORGE R. BLUMENTHAL

University of California Observatories/Lick Observatory, Board of Studies in Astronomy and Astrophysics, University of California, Santa Cruz, CA 95064

AND

S. M. FABER

University of California Observatories/Lick Observatory, Board of Studies in Astronomy and Astrophysics, University of California, Santa Cruz, CA 95064

Received 1992 June 29; accepted 1992 December 18

ABSTRACT

Using a simple analytic model of the response of dark matter halos to the dissipative infall of the luminous material to form an exponential disk, we explore the dependence of the final rotation curves on all the relevant parameters: the ratio $F \equiv M_b/M$ of the dissipative baryonic mass M_b to the total galaxy mass M including dark matter; the ratio b/R of the disk exponential scale length b to the truncation radius R (beyond which infall can be neglected); the core radius r_{core} of the isothermal halo in the absence of dissipation; and the dimensionless angular momentum parameter $\lambda \equiv J|E|^{1/2}G^{-1}M^{-5/2}$ (where J and E are the total angular momentum and energy of the galaxy). We explore in particular the final rotation curves expected in the tidal torque theory of angular momentum, in which $\langle\lambda\rangle \approx 0.05$. For $\lambda = 0.05$, we find the final rotation curve to be flat when the gravitational effect of the infalling baryonic material on the dark halo is included and if $F \approx 0.05$, the value suggested by nucleosynthesis constraints if the Hubble parameter $H_0 \approx 50 \text{ km s}^{-1} \text{ Mpc}^{-1}$. Also, the mass inside a “Holmberg” radius $R_H \equiv 4.5b$ is about half luminous and half dark as observations indicate. These results are quite insensitive to r_{core} provided it is sufficiently large, and are characteristic of any theory in which $\langle\lambda\rangle \approx F$. The key results are that for $F \approx 0.05$ the dispersion in λ expected in the tidal torque theory, $0.02 \leq \lambda \leq 0.1$, (a) leads to rotation curves for bright galaxies whose systematics are much like those of the galaxies for which H I data are available when consistent baryonic disk scale lengths are used throughout; and (b) the mass inside R_H shows a spread of values consistent with observations except possibly for the smallest galaxies, which may have suffered significant gas loss. With this range of λ -values, the distribution of outer rotation curve slopes for a given maximum rotation velocity is inconsistent with the data if F is substantially larger or smaller than 0.05, or if r_{core}/R is substantially smaller than 0.2.

Subject headings: dark matter — elementary particles — galaxies: formation — galaxies: kinematics and dynamics

1. INTRODUCTION

The formation of structure in the universe is most elegantly explained by the gravitational instability theory, in which small inhomogeneities in the distribution of matter are amplified during the expansion of the universe and eventually collapse to form bound structures. Inflation provides one theoretical basis to explain the origin of such inhomogeneities from microphysics, and their existence naturally explains the recent observation of anisotropies in the microwave background radiation (Smoot et al. 1992). When hierarchical clustering from small to large scales occurs, the angular momentum of galaxies naturally arises from the inevitable tidal interaction between a protogalaxy and its nearest neighbors as they expand and collapse (Peebles 1969).

The modern gravitational instability theory of galaxy formation was initiated in the papers of White & Rees (1978) and

Fall & Efstathiou (1980). According to White & Rees, protogalaxies comprised a mixture of dissipationless dark matter (which they supposed most probably to consist of Population III stars or their remnants, but which could just as well be nonbaryonic) and dissipative baryonic material, roughly in the mass ratio 10:1. As an individual protogalaxy separated from the Hubble expansion, the dark matter relaxed violently into roughly isothermal dark halos. In the process, the dissipative material was heated to the halo virial temperature; it then cooled, collapsed, and fragmented into the stars we see today in the bright galactic spheroids and disks. Fall & Efstathiou (1980) considered the origin of the angular momentum of disk galaxies in this scenario. They showed that the small initial value of the dimensionless angular momentum λ generated in protogalaxies by tidal torques could result in the large λ of galactic disks if the disk material contracted by roughly an order of magnitude in radius during its dissipative collapse within dissipationless halos, which is just the contraction factor expected for a ratio of dark to luminous matter of 10:1. Blumenthal et al. (1984, hereafter BFPR) argued that this general

¹ UCO/Lick Observatory Bulletin No. 1248.

picture of galaxy formation would apply in the cold dark matter theory.

The high-quality observational data now available on disk galaxy rotation curves demands quantitative explanation. The data (see Casertano & van Gorkom 1991, Broeils 1992, and references therein) present several challenges to theory: the “conspiracy” problem, clarification of the initial conditions needed for the rotation curves observed, and accounting for the regularities found in the variation of rotation curve shape and amplitude with other properties of spiral galaxies or their environments.

1.1. The “Conspiracy” Problem (Bahcall & Casertano 1985)

Although there is a transition at a few exponential disk scale lengths b between the inner region where luminous matter is gravitationally dominant and the outer region where the dark matter dominates, there is usually no significant feature marking this transition in the rotation curves of circular velocity $v(r)$ versus radius. Indeed, for many galaxies, $v(r)$ is remarkably constant from roughly a disk scale length b , through the transition region just mentioned, which roughly corresponds to the optical edge of the galaxy (= the Holmberg radius R_H), out to the largest radii at which H_I radio observations of $v(r)$ extend (e.g., out to $\lesssim 11b$ for NGC 3198; van Albada et al. 1985). Note that the issue here is the absence of a feature to mark the transition, not the flatness of the rotation curve. Another way to stress the conspiracy problem is to point out that from a given rotation curve it is not possible to unambiguously separate the dark and luminous components, *regardless of whether the rotation curve falls or rises through the optical radius*. This suggests the existence of a physical mechanism that is responsible for continuity between disk and halo mass distributions.

An earlier paper by the present authors (Blumenthal et al. 1986, hereafter BFFP) showed that this continuity could be the result of the gravitational pulling in of the dark matter during the contraction of the dissipative disk material if three conditions are met: (1) the dissipative baryonic fraction $F \equiv M_b/M$ and (2) the ratio b/R of the disk exponential scale length b to the infall truncation radius R are both $= O(0.1)$, and (3) the core radius r_{core} of the dark halo in the absence of dissipation is large: $r_{\text{core}}/R \gtrsim 0.5$. Blumenthal (1988) showed how the condition on b/R can be replaced by a constraint on the initial angular momentum λ . (Gas infall to the disk is assumed not to occur for $r > R$. More precise definitions of R and r_{core} are given in § 2.) As discussed below, these are precisely the conditions implied by observational and theoretical constraints.

1.2. Initial Conditions for Flat Rotation Curves

The main burden of the present paper is to show that if condition (1) is met, condition (2) naturally arises from the magnitude of protogalactic angular momentum λ due to tidal torquing, to a large extent independently of condition (3). Furthermore, we show that the expected range of values of λ , and therefore of b/R , leads to variations in rotational profiles quantitatively much like those observed.

Observational evidence, reviewed in BFPR, supports the validity of the first condition. Furthermore, if F is assumed to be a universal constant, it is most plausible that $F \approx \Omega_b/\Omega$, where as usual Ω and Ω_b are the total density and the density of baryons, both in units of critical density. The most recent nucleosynthesis constraints (Olive et al. 1990; Walker et al. 1991) imply that $0.010 \leq \Omega_b h^2 \leq 0.016$; i.e., for $H_0 \approx 50 \text{ km}$

$\text{s}^{-1} \text{Mpc}^{-1}$, $\Omega_b \approx 0.05$. Hence, $F \approx 0.05$ in this case if the universe has a critical density of matter, as suggested by recent large-scale observations. These recent results suggesting that $\Omega \approx 1$ include a combined analysis of the *IRAS* density field and all the available galaxy peculiar velocities (Dekel et al. 1993), and also an attempt to reconstruct Gaussian initial fluctuations from the peculiar velocities, which works for $\Omega \approx 1$ but fails for $\Omega \lesssim 0.3$ (Nusser & Dekel 1993).

It is not yet clear what the conditions are for the validity of (3). Early N -body simulations of protogalactic properties in cosmological simulations (Frenk et al. 1985; Quinn, Salmon, & Zurek 1986) did not have enough resolution to investigate protogalactic values of r_{core} . Recently, however, higher resolution simulations have become available (Dubinski & Carlberg 1991; Warren et al. 1992). These simulations indicate that cold dark matter halos have a universal profile, well approximated by a Hernquist (1990) profile $\rho(r) \propto r^{-1}(r+a)^{-3}$, which has a central density spike (i.e., $r_{\text{core}} \approx 0$). We discuss below why this would lead to serious conflict with observations.

1.3. Systematics of Observed Rotation Curves

Detailed data have become available in recent years on both the morphology and rotation of spiral galaxies, and systematic regularities have been pointed out to emerge from these observations. One approach has been to analyze galactic rotation in the inner parts of galaxies, typically out to distances $\lesssim R_H$. Burstein & Rubin (1985) found optical rotation curves in a sample of some 50 spiral galaxies to have a range of shapes. This range was characterized by three typical shapes called “families.” Furthermore, rotation curve shapes were found not to correlate (in a statistically significant way) with any intrinsic property of the galaxy (Burstein & Rubin 1985), but a correlation with environment was found (Whitmore, Forbes, & Rubin 1988). An analysis based on more recent data, however, does not find such correlation (Amram et al. 1993). Also, it has been claimed recently that galactic rotation curves do show a strong variation with luminosity (Persic & Salucci 1991; Persic, Ashman, & Salucci 1991).

Another important property of the distribution of dark and luminous matter found from optical rotation curves is that, typically, the ratio of the total dark mass to total luminous mass within the Holmberg radius is roughly unity (Burstein & Rubin 1985), but values spread by a factor of ≈ 3 (Kent 1986; Athanassoula, Bosma, & Papaioannu 1987).

A different approach has been recently adopted by Casertano & van Gorkom (1991). They have studied the rotation of galaxies for which radio (21 cm) as well as optical rotation curves are available, and they analyze the systematic variations in the outer rotation curves (from $\frac{2}{3}$ of the optical radius out to the last measured point, typically $8b$ – $10b$). They find that the slope of this outer rotation curve correlates with disk scale length, and anticorrelates with maximum rotational velocity (i.e., slowly rotating galaxies have rising rotation curves, rapidly rotating galaxies have falling ones). Broeils (1992) does a similar analysis of a different set of galaxies, including several for which radio data has recently become available. He finds that the correlations claimed by Casertano and van Gorkom apply only to the more slowly rotating galaxies ($v_{\text{max}} < 180 \text{ km s}^{-1}$).

In this paper we present the systematics of the rotation curves that emerge from the infall model (BFFP) to clarify the origin of the variations to be expected. We then attempt a

comparison with observations. Here we shall address the question of the ratio of luminous to dark mass inside the Holmberg radius, and then relate this to all the data considered by Casertano and van Gorkom and by Broeils. Because only the outer part of the rotation curve, beyond about $3b$, is relevant, these data are especially suited to analyze the disk-halo interplay without introducing the complication of bulges. We have considered the effect of introducing bulges and indeed find that their presence does not affect the shape of the rotation curve beyond $3b$.

We find that, in the infall model, the ratio of dark to luminous mass inside the Holmberg radius is indeed of order unity if $F \equiv M_b/M = O(0.1)$ (our condition [1]), more or less independently of whether $r_{\text{core}}/R \gtrsim 0.5$ (condition [3]). Moreover, values of this ratio spread by a factor $\lesssim 3$ as a result of the spread in values of λ indicated by N -body simulations.

We then point out that the anticorrelation of rotation curve slope and maximum velocity found by Casertano and van Gorkom is driven largely by small galaxies ($v_{\text{max}} \lesssim 80 \text{ km s}^{-1}$), for which the visible matter is largely H I rather than stars. In order to compare with our model predictions, it is more reasonable to use the H I disk scale length b_{HI} rather than the optical scale length. When we compare the model to the data over the corresponding ranges of b_{HI} , we find good agreement of rotation curve slopes. The ratio of visible matter (optical plus H I) to dark matter is however lower in these galaxies than in larger ones; most likely there has been significant gas loss (Dekel & Silk 1986), resulting in smaller effective values of F .

Taking all the available data into account, we find that there is little or no correlation between rotation curve slope and maximum velocity, as expected in the theoretical model if F is a universal constant, and that the range of values of the slopes of the observed rotation curves agrees with the theoretical range of values. We also discuss the correlation of rotation curve slope with disk size. We point out that the correlation is qualitatively a correlation with λ , as anticipated by Casertano and van Gorkom, but the physics of the truncation radius R becomes crucial to understand it quantitatively. We briefly discuss also how this relates to the understanding of the Tully-Fisher relation.

This paper is organized as follows. We present our model of the response of the dark matter halo to baryonic infall in § 2 and extensively discuss the properties of the rotation curves that emerge. We then present a discussion of the comparison to the data in § 3. Finally, § 4 summarizes our conclusions.

2. THE ADIABATIC MODEL FOR INFALL

2.1. Nature of the Model

Considerable effort has been devoted to the study of the formation of protogalaxies in the gravitational instability model in order to determine the expected ranges of the parameters describing their physical properties, such as matter distribution and dimensionless angular momentum λ . To relate these protogalaxies to real galaxies, one must quantify the effect of the dissipational infall of the visible matter on the mass distribution of the dark halo, so that, for example, the properties of the rotation curves of disk galaxies can be deduced from those of the protogalaxies they evolved from and can be compared with the observations.

BFFP describe a convenient approximate analytical model which has been checked by numerical simulations (Barnes

1987; Oh 1990) for calculating the radial redistribution of the dissipationless halo matter of a protogalaxy when its dissipational (visible) matter falls in toward the center. One starts by noting that for a particle moving in a periodic orbit $\oint p dq$ is an adiabatic invariant, where p is the canonical momentum conjugate to the coordinate q . Thus, for particles moving in circular orbits about a spherically symmetric mass distribution, the adiabatic invariant is $rM(r)$ provided that $M(r)$, the mass inside the orbital radius r , changes slowly compared with an orbital time (Steigman et al. 1978; Zel'dovich et al. 1980; Ryden & Gunn 1987; Ryden 1988). For purely radial orbits, $r_{\text{max}} M(r_{\text{max}})$ is also an adiabatic invariant provided that $M(r)$ varies in a self-similar fashion.

Consider now a spherically symmetric protogalaxy that consists of a fraction $F \ll 1$ of dissipational baryons and a fraction $1 - F$ of dissipationless dark matter particles which will constitute the halo. Collapsed protogalaxies are not likely to be spherically symmetric. In fact, collapsed protogalaxies extracted from N -body simulations are found to be triaxial in general (Dubinski & Carlberg 1991; Warren et al. 1992). However, we shall be interested in axially averaged properties of disk galaxies, for which the assumption of spherical symmetry should not be a seriously deficient approximation because an overall correction is irrelevant to the shape of a rotation curve, and the variation of triaxiality with radius is rather small (Dubinski & Carlberg 1991; Warren et al. 1992). Axially averaged rotation curves from two-dimensional velocity fields in disk galaxies indeed agree quite well with one-dimensional, slit rotation curves (Amram et al. 1993). We shall assume here that the observed properties of slit rotation curves are indeed a fair representation of those of the average velocity profile.

We assume that the dissipational baryons and the halo particles are well mixed initially (i.e., the ratio of their densities is F throughout the protogalaxy). Define a truncation radius R beyond which it will be assumed that no dissipation takes place; thus the total mass inside R is constant in all subsequent discussion. Clearly, R cannot exceed the maximum radius within which the gas can cool in less than the age of the universe. If we assume that the gas is at the virial temperature and well mixed with the dark matter before cooling (i.e., the ratio of their densities is F throughout the protogalaxy), then $R_{\text{cool}} \approx 100(F/0.1)^{1/2} h^{-1/2} (v_c/300 \text{ km s}^{-1})^{1/2} \text{ kpc}$ for an age of $6.6 \times 10^9 h^{-1}$ years, where h is the Hubble constant in units of $100 \text{ km s}^{-1} \text{ Mpc}^{-1}$, v_c is the circular velocity at distance R_{cool} , and we have taken a cooling function for primordial gas $\Lambda(T) \approx 10^{-27} \text{ ergs s}^{-1} \text{ cm}^3 (T/\text{K})^{1/2}$ (Rees & Ostriker 1977, White & Frenk 1991) and assumed that the initial mass distribution is that of an isothermal sphere with $r_{\text{core}}/R = 0.5$. Note, however, that all the results for dimensionless quantities that we discuss below depend only on the existence of some limiting radius R , not on the assumption that $R = R_{\text{cool}}$. The real situation is undoubtedly more complex (see, e.g., Katz & Gunn 1991).

Since there is more phase space for nearly circular orbits than for nearly radial orbits, we shall make the approximation that the dark matter particles move in circular orbits about the protogalaxy center with almost randomly oriented angular momentum vectors. (We assume the protogalaxy has a small initial angular momentum, as discussed below.) Thus, as the baryons dissipatively cool and fall in to the center forming a disk, a dark matter particle initially at radius r_i will move in to radius $r < r_i$. The adiabatic invariant for such a particle

implies that

$$r[M_{\text{disk}}(r) + M_{\text{halo}}(r)] = r_i M_i(r_i), \quad (1)$$

where $M_i(r_i)$ is the initial total mass distribution, $M_{\text{disk}}(r)$ is the final mass distribution of dissipational baryons, and $M_{\text{halo}}(r)$ is the final distribution of dissipationless halo particles. If we assume that the orbits of the halo particles do not cross, then

$$M_{\text{halo}}(r) = (1 - F)M_i(r_i), \quad (2)$$

and equations (1) and (2) can be used to calculate the final radial distribution of the halo particles once $M_i(r_i)$ and $M_{\text{disk}}(r)$ are given. If the dissipational mass fraction $F \ll 1$, then, for a halo particle not too near the center of the protogalaxy, the mass interior to its orbit will undergo a small fractional change in one orbital period, even if dissipation occurs rapidly. Therefore, the adiabatic invariant given in equation (1) is expected to be a good approximation for all but the innermost halo particles. *In the inner region $r \lesssim b$ the baryonic mass is dominant anyway, so the failure of (1) there is not very relevant to the shape of the rotation curve.*

In order to use the adiabatic invariant, the initial mass distribution $M_i(r_i)$ must be assumed to be an equilibrium configuration. We shall assume that the initial protogalaxy relaxes to an isothermal sphere with core radius (Chandrasekhar 1960)

$$r_{\text{core}}^2 = \frac{3\langle\sigma^2\rangle}{4\pi G\rho_0}, \quad (3)$$

where σ is the one-dimensional velocity dispersion and ρ_0 is the central density. This initial state is motivated by the expectation that particles in the inner regions of virialized protogalaxies would have gone through fairly chaotic changes of the local gravitational potential for extended periods of time, and thus the conditions for violent relaxation would be met (Lynden-Bell 1967; Shu 1978), which yields an isothermal sphere as the equilibrium configuration. For example, this initial state was found to be a good approximation (in the absence of dissipation) to the equilibrium radial mass distribution of an isolated, expanding protogalaxy that consisted of a large number of "clouds" initially in pure Hubble flow and distributed inside a truncated sphere with a Poisson distribution (see BFFP). In reality, one expects some dissipation to occur before a protogalaxy has fully virialized, but this does not substantially change the results (BFFP; Flores et al. 1986). Also, since dissipation occurs within a finite radius R , for small r_{core}/R we take into account the possibility that the initial halo rotation curve fall with distance, as is the case for halos in cosmological N -body simulations (Frenk et al. 1985; Quinn et al. 1986).

As BFFP first emphasized, large values of the core radius, $r_{\text{core}}/R \lesssim 0.5$, are needed for baryonic infall to produce mass distributions with flat rotation curves. Such large values would arise naturally if protogalaxies had a substantial amount of kinetic energy at maximum expansion, and they found this to be the case for the isolated expanding protogalaxy. However, one should really simulate a large expanding region from which collapsed protogalaxies could be extracted to more accurately know r_{core}/R . Recently, such simulations have been carried out with very high resolution for cold dark matter (Dubinski & Carlberg 1991; Warren et al. 1992). In these simulations dark matter halos end up with very small values of r_{core} . As we shall discuss below (see also Flores & Primack 1993), such halos lead to serious conflict with observed rotation

curves once the infall of baryonic material within such halos is taken into account.

For a spiral galaxy, the final radial mass distribution of the baryons is constrained by the initial angular momentum of the protogalaxy. Here, the final mass distribution of the disk will be assumed to be

$$M_{\text{disk}}(r) = \mathcal{M}_{\text{disk}}[1 - (1 + r/b)e^{r/b}], \quad (4)$$

which is the radial mass distribution of a thin disk of mass $\mathcal{M}_{\text{disk}}$ whose mass surface density

$$\mu_{\text{disk}}(r) = \frac{\mathcal{M}_{\text{disk}}}{2\pi b^2} e^{r/b} \quad (5)$$

decrease exponentially with scale length b . Such is the surface brightness profile of spiral galaxies (Freeman 1970), and since there is no evidence of radial variations in the mass-to-light ratios of spiral disks (see, e.g., van der Kruit 1990; Gilmore, King, & van der Kruit 1990), we shall assume this to be the disk mass profile as well. Numerical simulations (Oh 1990) indicate that the flattening of the distribution of baryons does not appreciably distort the halo from spherical symmetry. Thus, it is a reasonable approximation to assume the baryonic mass distribution to be spherical when using equation (1), and this has been done throughout this paper. Note, however, that velocity profiles will be calculated for real disks (see eq. [9] below).

2.2. Relation of Infall to Initial Angular Momentum

It is usual to describe the angular momentum, J , of a protogalaxy in terms of a dimensionless quantity

$$\lambda \equiv \frac{J|E|^{1/2}}{G\mathcal{M}^{5/2}}, \quad (6)$$

where \mathcal{M} is the total mass of a protogalaxy with total energy (gravitational plus kinetic) E . More than 20 years ago, Peebles (1959; see also Hoyle 1949) showed that, in the gravitational instability theory, galaxies like our own would acquire the right amount of angular momentum through tidal interaction with nearest neighbor protogalaxies as they expanded and collapsed. To the extent that the Galaxy could be considered typical in its angular momentum, Peebles's calculation showed that the mean angular momentum would be $\langle\lambda\rangle \approx 0.08$, but a wide distribution would be expected. Because the maximum rate of transfer of angular momentum between protogalaxies occurs at about the time the protogalaxies separate from the Hubble expansion of the universe, an analytic treatment of the process is very difficult, and N -body simulations are needed. Using such simulations, Efstathiou & Jones (1979) found a mean angular momentum $\langle\lambda\rangle \approx 0.07$, with a dispersion $\Delta\lambda \approx 0.03$. Barnes & Efstathiou (1987) found from higher resolution simulations that $\langle\lambda\rangle \approx 0.05$, quite independently of the shape of the power spectrum of density fluctuations, and that the λ -distribution is broad with $\lambda = 0.02$ – 0.1 for approximately 80% of the groups identified in the simulation. In this paper we shall use $\langle\lambda\rangle = 0.05$ as a fiducial value, and explore the effects of variations in λ on galactic rotation curves. In particular, we shall see that for the range of λ 's expected in the tidal torque theory, $\lambda = 0.02$ – 0.1 , the final rotation curves exhibit systematic variations that quantitatively agree with those of real galaxies. (Note that, in our model, it is only the λ of the matter inside the truncation radius R that matters; we assume that this also has essentially the same λ -distribution.)

Fall & Efstathiou (1980) first calculated how the amount of infall of the disk material is related to the initial angular momentum λ of a protogalaxy containing both dissipational and dissipationless material. They assumed that the formation of a disk involved no transfer of angular momentum between the disk and halo components. They also took a specific form for the halo density distribution, a stiff halo, which they assumed was unaffected by the dissipational infall of the disk material. The range of halos they considered included only rather flat rotation curves.

Using the adiabatic invariant, equation (1), it is straightforward to relax the stiff-halo assumption of Fall & Efstathiou (1980). For a thin exponential disk without a halo, roughly half of the angular momentum is contained by the outside 25% of the mass. Therefore, the calculation of the disk angular momentum involves mostly the region where the dark matter distribution can be reliably determined by the adiabatic invariant approximation.

Consider a protogalaxy with core radius r_{core} , truncation radius R , and dissipational baryonic fraction F . If the dissipational material settles to a disk with mass distribution given by equations (4) and (5), then the angular momentum of the thin disk is given by

$$J_{\text{disk}} = 2\pi \int_0^\infty r dr \mu_{\text{disk}}(r) v(r). \quad (7)$$

The circular velocity $v(r)$ is given by

$$v^2(r) = r[g_{\text{disk}}(r) + g_{\text{halo}}(r)]. \quad (8)$$

The inward acceleration of an exponential disk is given by

$$g_{\text{disk}}(r) = \frac{G\mathcal{M}_{\text{disk}}}{b^2} \left(\frac{r}{2b} \right) \left[I_0 \left(\frac{r}{2b} \right) K_0 \left(\frac{r}{2b} \right) - I_1 \left(\frac{r}{2b} \right) K_1 \left(\frac{r}{2b} \right) \right], \quad (9)$$

where I_n and K_n denote modified Bessel functions of order n (Freeman 1970). The acceleration due to the halo is

$$g_{\text{halo}}(r) = GM_{\text{halo}}(r)/r^2, \quad (10)$$

where $M_{\text{halo}}(r)$ is determined by iteratively solving equations (1) and (2). If we assume no transfer of angular momentum between disk and halo particles, then

$$J_{\text{disk}}/\mathcal{M}_{\text{disk}} = J_{\text{halo}}/\mathcal{M}_{\text{halo}}, \quad (11)$$

and the total angular momentum of the protogalaxy is

$$J = J_{\text{disk}}/F. \quad (12)$$

Hence λ for the protogalaxy is simply related to b . The assumption of no transfer of angular momentum, on the other hand, may appear unwarranted in view of results from numerical simulations (Frenk et al. 1985; Quinn et al. 1986; Barnes & Efstathiou 1987), where it was found that a substantial amount of angular momentum is transferred from the inner to the outer parts of developing dissipationless halos. However, this does not necessarily imply transfer of angular momentum between dark and visible components. Moreover, the transfer of angular momentum within the halo prior to virialization is not crucial here, since we take a range of values of λ corresponding to equilibrium configurations and we do not rely on, for example, invariance of the mass distribution as a function of specific angular momentum. Also, while recent simulations that include gas cooling (Katz & Gunn 1991) do show a signifi-

cant transfer of angular momentum between components, this occurs mostly between the spheroidal component and the dark matter. And, when star formation is included, it suppresses the formation of the dense knots of dissipated material whose torque is largely responsible for this angular momentum transfer (Katz 1992; L. Hernquist 1992, private communication). In any case, this should not be a serious issue when discussing disk-dominated spirals, as we do here.

Figure 1 shows how the amount of dissipative infall b/R is related to the initial angular momentum, λ . In Figure 1a we show the effect of assuming a stiff halo which does not respond to dissipative infall. The figure shows that the assumption of a stiff halo always leads to less infall, about 25% less infall for $\lambda = 0.05$. This occurs because a stiff halo produces a smaller rotation velocity for the disk at all radii, and therefore forces a larger disk radius if J_{disk} is conserved. Figure 1b shows how b/R versus λ depends on the baryonic fraction F . Here, smaller values of F again lead to less infall essentially because with small F the disk dynamics is dominated by the halo, which does not contract as much and therefore keeps the rotation speed low, again forcing a large disk radius. In the limit that $F \rightarrow 0$ the curve is expected to approach a limiting relation. Finally, Figure 1c shows how the relation between b/R and λ depends on the initial protogalaxy core radius r_{core} . Here, larger core radii produce less infall because a large core radius tends to keep rotation speeds in the inner halo low again forcing the disk radius to be large. As r_{core} becomes large compared to R , the initial protogalaxy density is nearly constant for $r < R$, and the curves become indistinguishable.

These results place in perspective the conclusions of BFFP, who found that flat rotation curves require $r_{\text{core}}/R \approx \frac{1}{2}$, $F \approx 0.1$, and $b/R \approx 0.05$. Figure 1 shows that such a value of b/R is consistent with the value $\lambda \approx 0.05$, precisely the typical value expected in the tidal torque theory of angular momentum in galaxies. Blumenthal (1988) found a similar result for λ by representing the flatness of rotation curves in a somewhat different fashion.

2.3. Systematics of Rotation Curves

The adiabatic invariant can also be used to calculate theoretical rotation curves, which we here investigate systematically for various values of the parameters.

Figure 2a shows the rotational velocity as a function of distance from the center, r/R , for fiducial values of F and r_{core}/R and for values of λ expected in the tidal torque theory. The figure shows that the dispersion in λ does not affect the rotation profiles in the outer parts beyond $r/R \lesssim 0.2$. However, the inner parts are substantially different for different λ 's. In Figure 2b and Figures 3a and 3b rotation velocity is plotted versus r/b , which is more easily related to observed galaxies. Figure 2b shows that both rising and falling rotation curves are expected beyond a couple of disk scale lengths. At the Holmberg radius of a galaxy, which roughly corresponds to $R_H = 4.5b$, the rotation curve can show a substantial decline for small λ because small λ leads to greater infall (smaller b/R) and a very centrally condensed mass distribution. Figure 3 shows the rotation profiles of the mass distributions that result after baryonic infall, for the typical value of dimensionless angular momentum $\lambda = 0.05$, and various values of F and r_{core}/R . One can see that for typical λ , flat rotation curves out to large radii arise for $F \lesssim 0.1$ and $r_{\text{core}}/R \lesssim 0.5$. Figure 3b also illustrates an important point that we have verified by an extensive search of

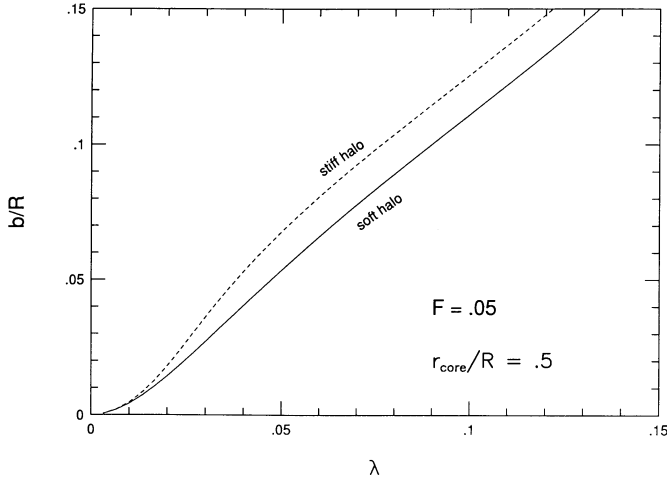


FIG. 1a

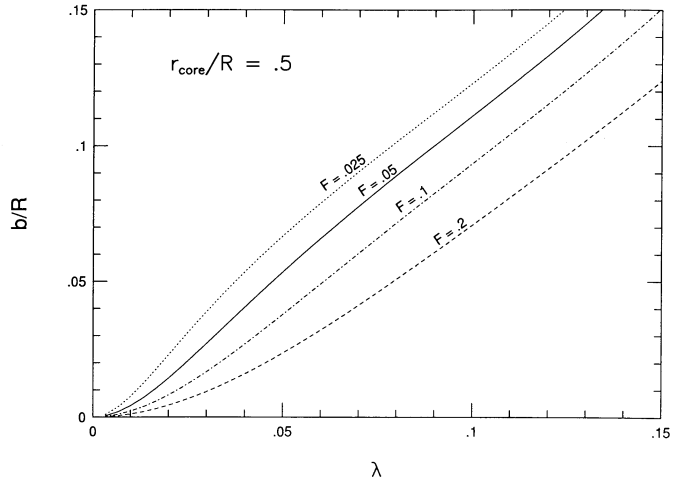


FIG. 1b

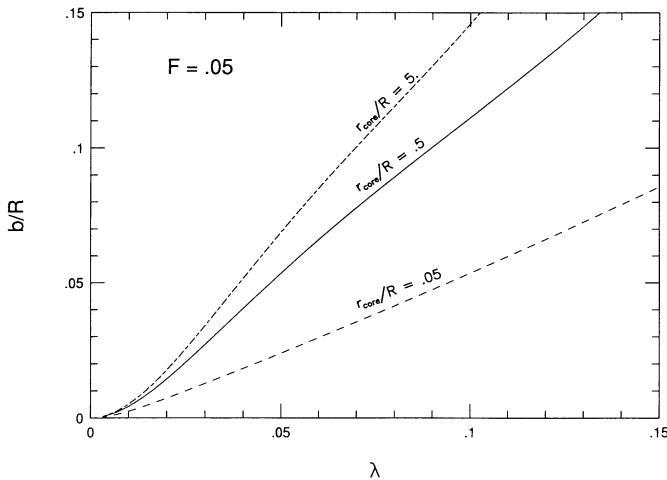


FIG. 1c

FIG. 1.—(a) Amount of dissipational infall vs. the dimensionless initial angular momentum λ for dissipational fraction $F = 0.05$ and $r_{\text{core}}/R = 0.5$. The ordinate is the ratio of the scale length b of the disk to the cutoff radius R of the initial isothermal sphere. The solid line represents the result when the halo responds to the baryonic infall; the dashed curve assumes no halo response to the infall of the disk. (b) Amount of dissipational infall vs. the dimensionless initial angular momentum λ for $r_{\text{core}}/R = 0.5$ and $F = 0.025, 0.05, 0.1$, and 0.2 . The variables have the same meanings as in Fig. 1a. (c) Amount of dissipational infall vs. the dimensionless initial angular momentum λ for $F = 0.05$ and $r_{\text{core}}/R = 0.05, 0.5$ and 5.0 . The variables have the same meanings as in Fig. 1a.

parameter space: *small initial core radii inevitably lead to falling rotation curves.* We will discuss these figures further below.

2.4. Relative Contributions of Disk and Halo

A notable property of the rotation curves of Figures 2 and 3, as was emphasized in BFFP, is that no feature is present in the rotation profile to separate the inner, disk-dominated region from the outer, halo-dominated region. The coupled motion of the two components, as the baryons fall into the center, avoids any noticeable separation of the two components. This would not have been the case had we considered the halo to be rigid, in which case a feature does appear in the rotation curve (see Flores 1987). Observationally, the absence of such a separation of the two components has been noted by Burstein & Rubin

(1985), Bahcall & Casertano (1985), and van Albada & Sancisi (1986). *We stress that the issue here is how well mixed the dark and luminous matter are, not the flatness of the rotation curve.*

These authors and others have also noted that there are roughly equal amounts of disk and halo matter interior to the optical radius of a galaxy, R_H . We have therefore plotted in Figure 4 the ratio of the rotational velocity due to the disk to that due to the halo matter at $r = 4.5b$, as a function of λ . The figure shows that for $F = O(0.1)$, this ratio is indeed close to unity for $0.02 \leq \lambda \leq 0.1$ over a wide range of values of r_{core} . Furthermore, for $F = 0.05$ and λ in this range, $(v_{\text{disk}}/v_{\text{halo}})^2$ at $r = 4.5b$ varies by roughly a factor of 3 about unity, as indicated by observations of large galaxies (Kent 1986; Athanassoula et al. 1987). For large F , the disk gives a relatively greater contribution to the rotational velocity because of the relatively larger central mass concentration. Therefore, the fact that $v_{\text{disk}} \approx v_{\text{halo}}$ at $r = 4.5b$ is a consequence of $F \sim \lambda \approx 0.05$.

2.5. Slope of the Outer Rotation Curve

Many authors have investigated the shapes of rotation curves within their optical radii (Burstein & Rubin 1985; Whitmore et al. 1988; Persic & Salucci 1991), finding that their outer slope between some inner point and the optical radius varies within a range about zero. The Holmberg radius of a galaxy corresponds to $R_H \approx 4.5b$ for a galaxy of central surface brightness of $20.5 \text{ mag arcsec}^{-2}$ in R-band, the typical value for bright spirals (Kent 1985). Thus, we characterize the outer rotation curve of model galaxies by a slope parameter defined by

$$\frac{\Delta v}{v} \equiv \frac{v(4.5b) - v(3b)}{v(3b)}. \quad (13)$$

In order to investigate the effect of variations in λ and r_{core} on the outer rotation profile of galaxies, we plot $\Delta v/v$ in Figure 5. In Figure 5a we see, once again, that for $r_{\text{core}}/R = 0.5$ and λ in the range 0.02 to 0.1, F must lie in the range 0.05 to 0.1 to give more or less flat outer rotation curves. For a given λ , F higher (lower) than this results in falling (rising) outer rotation curves. Figure 5b shows the effect of varying r_{core} and λ . For F fixed at 0.05 and $\lambda \leq 0.05$, the outer rotation curve is always falling, while for $\lambda \geq 0.05$, the outer rotation curve is always rising provided $r_{\text{core}} \geq 0.5$. Thus, rising (falling) rotation profiles would correspond to protogalaxies that had large (small)

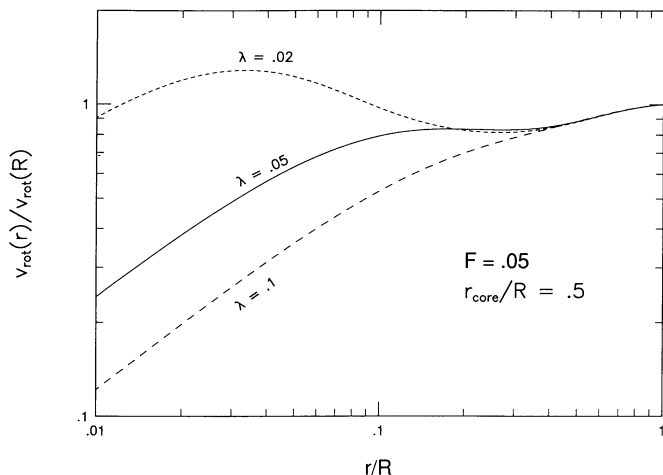


FIG. 2a

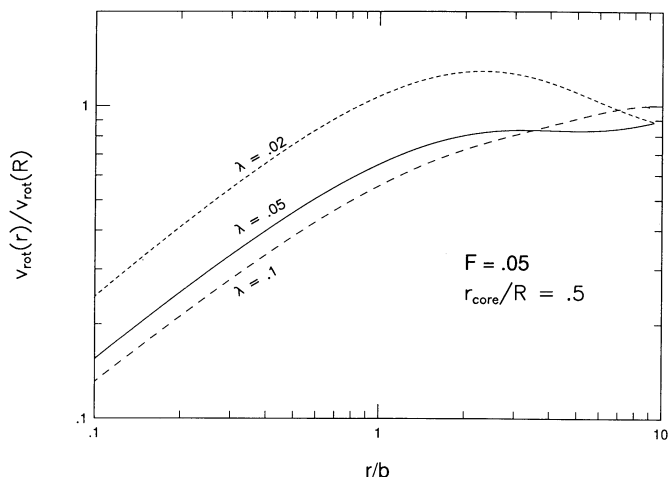


FIG. 2b

FIG. 2.—(a) Rotation curves, $v(r)/v(R)$ vs. r/R , for $F = 0.05$, $r_{\text{core}}/R = 0.5$, and several values of λ . (b) Same as Fig. 2a except that the abscissa is r/b , where b is the scale length of the disk.

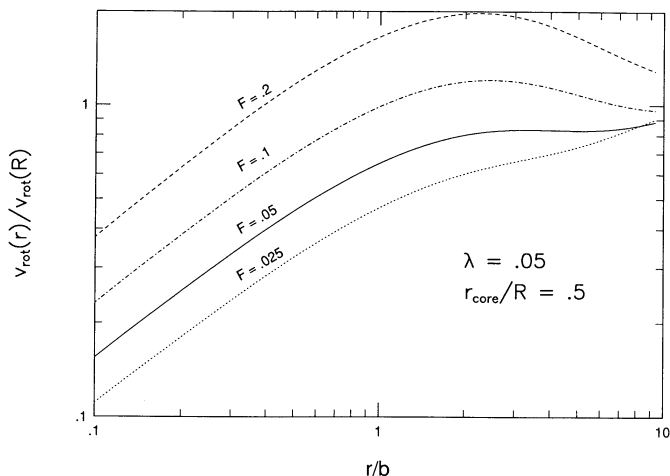


FIG. 3a

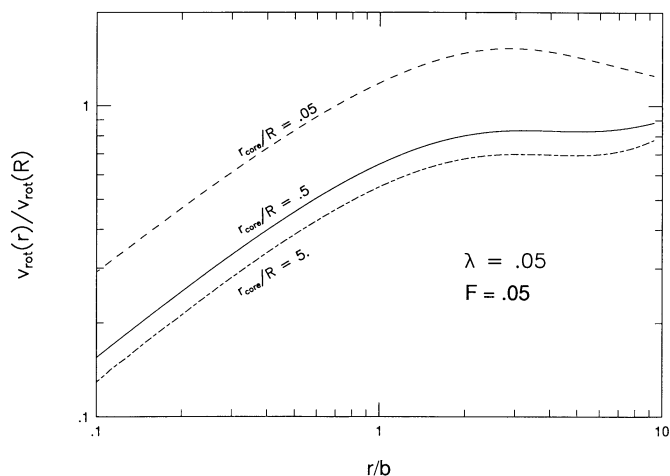


FIG. 3b

FIG. 3.—(a) Rotation curves for $\lambda = 0.05$, $r_{\text{core}}/R = 0.5$, and several values of the dissipational fraction F . (b) Rotation curves for $\lambda = 0.05$, $F = 0.05$ and several values of r_{core}/R .

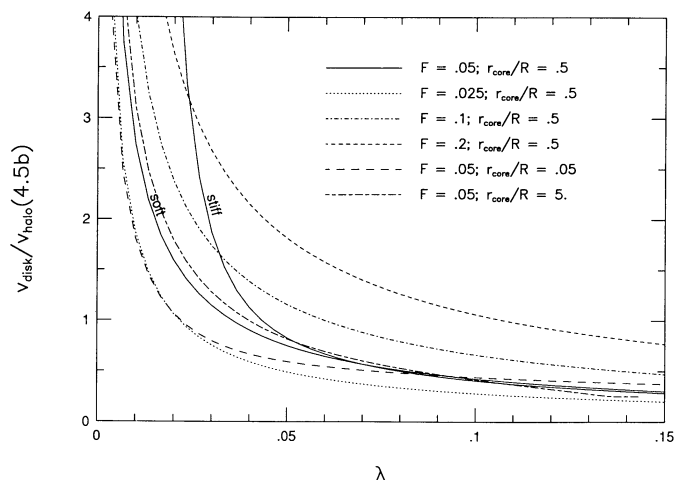


FIG. 4.—Ratio of the disk to halo contributions to the rotational velocity at $r = 4.5b$ vs. the angular momentum λ for various values of the dissipational fraction F and the initial core radius r_{core} .

angular momentum λ . Searching parameter space, we find that for $F \gtrsim 0.15$ only falling rotation profiles are possible, i.e., $v(4.5b) < v(3b)$ for $0.02 \leq \lambda \leq 0.1$ and any value of r_{core}/R . Likewise, for $F \lesssim 0.02$ only rising rotation profiles arise, i.e., $v(4.5b) > v(3b)$, because of the absence of a central mass concentration.

An important feature of Figure 5b is the fact that small core radii lead to falling rotation curves, and this we also find to be true outside the optical radius. As mentioned before, recent high-resolution simulations of the formation of cold dark matter halos (Dubinski & Carlberg 1991; Warren et al. 1991) indicate a very small core radius. We have calculated rotation curves in the case of gas infall within a dark matter halo with a Hernquist (1990) type profile and indeed find that only falling rotation curves result, even if the profile is modified to fall off like that of an isothermal sphere in the outer parts. This is certainly inconsistent with the data discussed below. We have also analyzed the rotation curve of the dwarf galaxy DDO 154 (Carignan & Freeman 1988), which is dark matter dominated

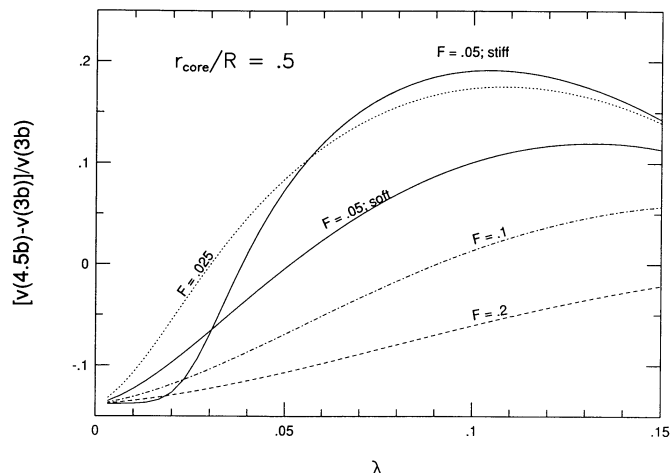


FIG. 5a

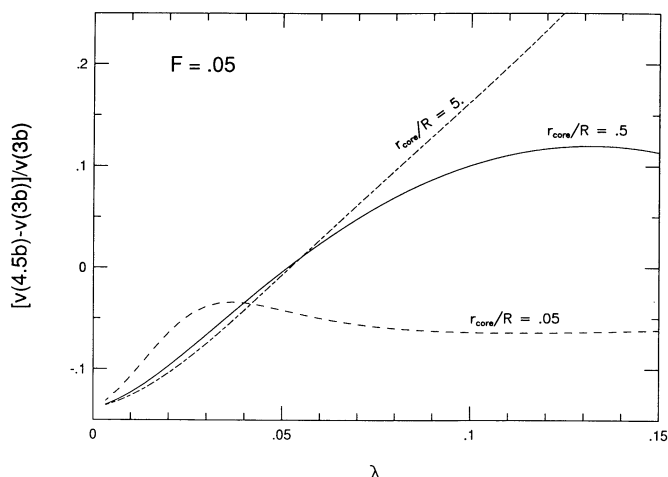


FIG. 5b

FIG. 5.—(a) Relative increase in rotation velocity between $r = 3b$ and $r = 4.5b$ vs. λ for $r_{\text{core}}/R = 0.5$ and several values of F . For comparison, a pure exponential disk has $[v(4.5b) - v(3b)]/v(3b) \approx -0.14$. (b) Same as Fig. 5a, but for $F = 0.05$ and various values of r_{core}/R .

at all radii, and also find it to be inconsistent with such a profile. (See also Flores & Primack 1993.)

3. DISCUSSION

The rotation curves we have presented here show much similarity with those of real spiral galaxies, and their qualitative systematic variations appear plausible. The picture that emerges from the figures we have just discussed is that these systematic variations could arise from the dispersion in the angular momentum of protogalaxies that have a universal gas fraction F . In this section we attempt to quantitatively compare the model rotation curves to those of real galaxies.

The systematics of optically measured rotation curves inside their optical radius are well studied (Burstein & Rubin 1985; Whitmore et al. 1988; Persic & Salucci 1991). Unfortunately, these observations are typically restricted to a very limited radial range of only a few disk scale lengths, $r \lesssim 3.5b$. Within that range of distances, galactic bulges can have a considerable effect on the shape of the rotation profile. Therefore it is not clear to what extent systematic variations reflect the interplay of luminous and dark matter or simply the interplay of the bulge and disk of the galaxy, which might not be connected to the presence of dark matter.

Recently, Persic & Salucci (1991) have analyzed the rotation curves of a sample of 58 Sb–Sc galaxies, which they say should minimize the effect of the bulges (although many Sb galaxies have large bulges). They claim that the slope of the galactic rotation curve between roughly $2b$ and $3b$ strongly correlates with luminosity. The infall model we have discussed predicts no correlation for galaxies with rotational velocities $\gtrsim 100 \text{ km s}^{-1}$ if F is constant, since little or no global gas loss from energy input by supernovae would be expected to occur during galaxy formation (Dekel & Silk 1986). Our model (for $F = 0.05$ and $\lambda = 0.02\text{--}0.1$) also predicts that the slope Δ defined by Persic & Salucci between $2.2b$ and $3.2b$ would lie in the range -0.05 to 0.2 if no bulge is present (i.e., for a pure exponential disk). We have investigated whether a correlation between total luminosity and bulge-to-disk luminosity ratio could possibly reproduce Persic & Salucci's result, and find that the degree of correlation allowed by the data (Kent 1985; Simien & de Vaucouleurs 1986) cannot explain it.

However, in going back to the original data, we found that there are two problems in relating our model to the data discussed by Persic & Salucci (1991): (1) several of the rotation curves do not in fact extend out far enough to determine Δ between $2.2b$ and $3.2b$, and (2) many of the surface brightness profiles are not exponential. Either problem (1) or (2) give larger Δ . We found that, of those galaxies for which they quote a maximum rotation velocity $\geq 100 \text{ km s}^{-1}$, all those with $\Delta \geq 0.2$ have either or both of these problems; therefore we cannot conclude that these data are evidence against our model. Clearly, a larger sample of spirals with exponential disks and velocity data that extend at least out to $3b$ will be needed to test the validity of the model in this range of radii.

Here we shall concentrate on the outer rotation curve, $r \gtrsim 3b$, where the effect of bulges is negligible for $r_{\text{eff}}/b \leq 1.0$ and $M_{\text{bulge}}/M_{\text{disk}} \leq 2(L_{\text{bulge}}/L_{\text{disk}}) \leq 10$, the range for most spirals (Kent 1985; Simien & de Vaucouleurs 1986).

Casertano & van Gorkom (1991) have addressed the systematics of rotation curves well outside their optical radii for a sample of 28 galaxies for which there are both radio and optical rotation curve data plus surface photometry data. They analyze the logarithmic slope of the rotation curve, defined as the slope of the log-log plot of $v(r)$ χ^2 -fit to a straight line, as a function of various properties of the galaxy. The radial range is restricted to the region between an inner fiducial radius of $\frac{2}{3}$ of the optical radius and an outer radius given by the last point where there are radio data, about 8 scale lengths on average for the brighter galaxies in their sample. Since $\frac{2}{3}$ of the optical radius corresponds to 3 scale lengths for a galaxy of central surface brightness $20.5 \text{ mag arcsec}^{-2}$, we shall look at the logarithmic slope of model rotation curves in the radial range $r = 3b\text{--}8b$. The logarithmic slope of their bright galaxies is insensitive to whether the inner radius is restricted to 3 optical scale lengths or to $\frac{2}{3}$ of the optical radius (Casertano & van Gorkom 1991), and the slopes of the model rotation curves remain almost the same as the outer radius is varied from 8 to 10 scale lengths.

The first correlation discussed by Casertano & van Gorkom (1991, their Fig. 6) is logarithmic slope versus maximum velocity outside their inner fiducial radius. The find a steep decline in logarithmic slope as the maximum velocity increases. Broeils

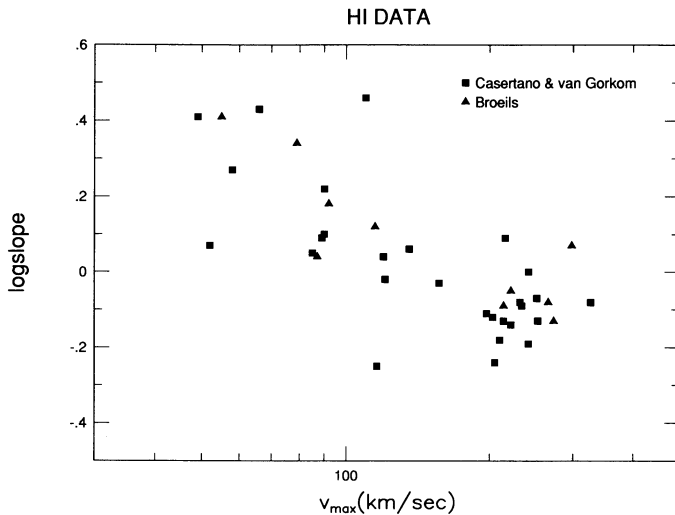


FIG. 6a

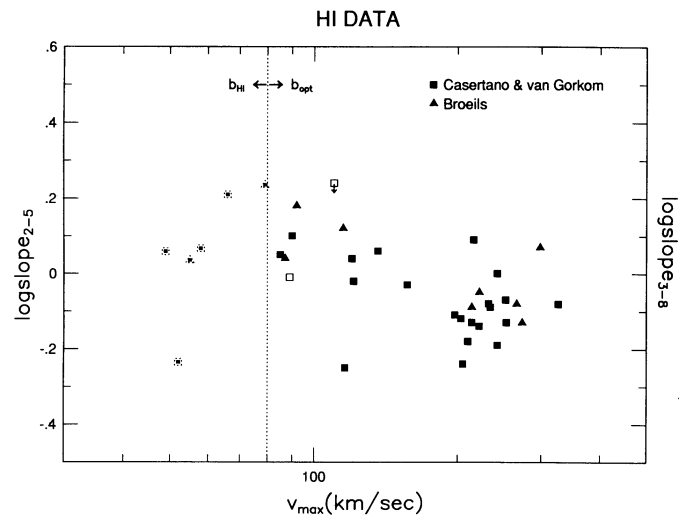


FIG. 6b

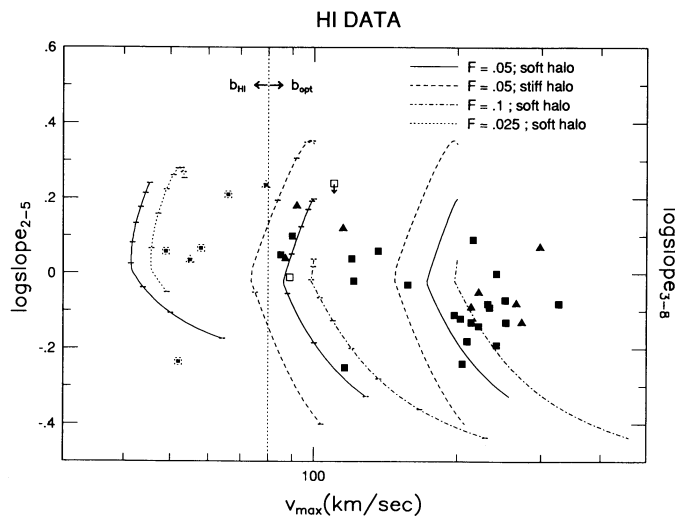


FIG. 6c

FIG. 6.—Logarithmic slope vs. maximal rotational velocity. (a) Data in Table 1, log of col. (3) vs. col. (4). This is all the data in Casertano & van Gorkom (1991), and all the additional data in Broeils (1992). Following these authors, galaxy logarithmic slope is calculated starting at $\frac{2}{3}R_{25}$ out to the most distant radius at which a velocity measurement is available. (b) Same data as in (a), reanalyzed over a fixed range of disk scale lengths based upon the dynamically dominant baryonic component, i.e., using the H I rather than optical scale length for galaxies to the left of the vertical dashed line. The H I scale lengths are given in Table 2. The logarithmic slope is again calculated out to the most distant velocity measurement point for all galaxies. For galaxies with $v_{\max} \leq 80 \text{ km s}^{-1}$ (to the left of the vertical dashed line) we calculate the slope starting at 2 H I scale lengths, i.e., for $r \geq 2b_{\text{H I}}$, and show their new position in the diagram by dot-outlined symbols. The rotation curves of these galaxies extend out to $\sim 5b_{\text{H I}}$. For galaxies with $v_{\max} \geq 80 \text{ km s}^{-1}$ we show the data as in panel (a), except for the open symbols which show the new position in the diagram of galaxies whose slopes change by more than 0.05 when calculated starting at 3 optical scale lengths from their centers. The rotation curves of these galaxies extend out to $\sim 8b_{\text{opt}}$ on average, but for the galaxy marked by the down arrow (NGC 247) it extends out to only $3.5b_{\text{opt}}$ and, therefore, its true slope in the distance range $3-8b_{\text{opt}}$ is probably much smaller. The point for NGC 4395 is omitted since there are no velocity measurements outside $3b_{\text{opt}}$. (c) Same as (b), with theoretical predictions overlain. The three sets of curves are the loci of model galaxies of constant mass, corresponding to $v(R) = 50, 100, 200 \text{ km s}^{-1}$, and varying λ . To the right of the vertical dashed line, the slope of model rotation curves is calculated in the distance range $3-8b$, whereas on the left it is calculated in the range $2-5b$. The ticks along the curves indicate model galaxies with values of λ differing by 0.01, starting with $\lambda = 0.02$ at the bottom; some of the higher λ tick marks overlap. All curves are drawn with $r_{\text{core}}/R = 0.5$, except for the $F = 0.025$ curve for which $r_{\text{core}}/R = 0.2$. The stiff halo curves unrealistically assume no halo response to the formation of the disk.

(1992) finds a similar correlation for low and intermediate luminosity galaxies. Both data sets are presented in Table 1 and plotted in Figure 6a, where the trend is obvious.

Our theory predicts no such trend, at least for large galaxies. It is quite apparent from Figures 2 and 3 above that the slope of the outer model rotation curve is most sensitive to variations of λ and F . No global gas loss from supernovae would be expected to occur during the formation of spiral galaxies with rotational velocities $\gtrsim 100 \text{ km s}^{-1}$ (e.g., Dekel & Silk 1986). Thus, large gas disks that form within galactic halos generated by adiabatic perturbations should have a universal gas fraction F . However, gas disks of fixed mass would form in galactic halos of varying angular momentum λ , and therefore would exhibit varying logarithmic slopes at fixed luminosity. The range of values of the logarithmic slope, on the other hand, is not predicted to vary as a function of luminosity.

What about smaller galaxies? Our model calculations give the rotation curve versus the radius in units of disk scale length. The logarithmic slope data plotted in Figure 6a is from $\frac{2}{3}$ of the optical radius to the last measured velocity, but for all the galaxies in Figure 6a with $v_{\max} \leq 80 \text{ km s}^{-1}$, it is very likely that the dynamically dominant baryonic component is not stars but neutral gas (H + He), given their high gas mass-to-blue-light ratios and their colors. In order to compare data on these galaxies with our model, it is therefore necessary to consider the rotation curve over a fixed range of H I rather than optical scale lengths. In Figure 6b we have replotted the data this way. Since the available data do not extend beyond about $5b_{\text{H I}}$ for the galaxies with $v_{\max} \leq 80 \text{ km s}^{-1}$, for these galaxies we plot the logarithm of the slope for $r \geq 2b_{\text{H I}}$. This choice of inner radius is dictated by the desire to have many velocity measurements outside the inner radius, and to avoid the inner parts where the stellar disk component becomes important. The outer H I surface density profile is reasonably well fit by an exponential profile, with scale lengths $b_{\text{H I}}$ given in Table 2. The inner profiles typically level off at surface densities smaller than predicted by the exponential fit, but we look at the slopes of rotation curves over an outer distance range where the effect of this is rather small. Only for two of these objects is the gas mass-to-blue-light ratio as low as 1, raising the concern that the stellar component might be equally important dynamically. However, for one of them (DDO 168) the light and the H I disk scale lengths are very similar, and for the other (NGC

TABLE 1
GALAXIES WITH H I ROTATION CURVE DATA IN ORDER OF INCREASING MAXIMAL ROTATIONAL VELOCITY

Name	b_{opt} (kpc)	logslope	v_{max} (km s ⁻¹)	Distance (Mpc)	$2R_{25}/9b_{\text{opt}}$	Source
DDO 154	0.5	0.41	49.	4.	0.68	CvG
NGC 2366	1.25	0.07	52.	3.3	0.56	CvG
DDO 168	0.9	0.41	55.	3.5	0.42	B
NGC 3109	1.35	0.27	58.	1.7	0.44	CvG
DDO 170	1.57	0.43	66.	14.6	0.33	CvG
NGC 1560	1.3	0.34	79.	3.0	0.74	B
NGC 300	1.8	0.05	85.	1.9	0.67	CvG
NGC 55	1.6	0.04	87.	1.6	1.2	B
NGC 4236	2.72	0.09	89.	3.2	0.60	CvG
NGC 4395	3.08	0.22	90.	4.5	0.59	CvG
UGC 2259	1.34	0.10	90.	9.8	0.63	CvG
NGC 5585	1.4	0.18	92.	6.2	0.75	B
NGC 247	2.72	0.46	110	2.5	0.49	CvG
NGC 1003	1.9	0.12	115.	11.8	1.1	B
NGC 7793	1.08	-0.25	116	3.4	0.88	CvG
NGC 925	4.24	0.04	120.	9.4	0.67	CvG
NGC 6503	1.72	-0.02	121.	5.9	0.58	CvG
NGC 2403	2.08	0.06	136	3.2	0.86	CvG
NGC 3198	2.52	-0.03	157	9.4	0.87	CvG
NGC 4013	2.27	-0.11	197.	11.8	0.65	CvG
NGC 2903	1.99	-0.12	203.	6.4	1.2	CvG
NGC 2683	1.2	-0.24	205.	5.1	1.0	CvG
NGC 3521	2.38	-0.18	210	8.9	1.0	CvG
NGC 2998	5.4	-0.09	214	67.4	1.2	B
NGC 5055	3.96	-0.13	214.	8.0	0.75	CvG
NGC 4258	5.22	0.09	216.	6.6	0.65	CvG
NGC 801	12.	-0.05	222.	79.2	0.67	B
NGC 5033	5.40	-0.14	222.	11.9	0.68	CvG
NGC 5907	5.90	-0.08	232.	11.4	0.51	CvG
NGC 4725	6.75	-0.09	234.	16.0	0.82	CvG
NGC 5371	4.35	-0.19	242.	34.8	1.1	CvG
NGC 7331	5.03	0.0	242.	14.9	0.91	CvG
NGC 224	5.4	-0.07	252.	0.7	0.64	CvG
NGC 4565	8.95	-0.13	253.	16.2	0.66	CvG
NGC 6674	8.3	-0.08	266.	49.3	0.80	B
NGC 5533	11.4	-0.13	273.	55.8	0.51	B
UGC 2885	13.	0.07	298.	78.7	1.1	B
NGC 2841	2.46	-0.08	326.	9.5	0.88	CvG

NOTES.—Columns list the galaxy (1) name, (2) optical scale length, (3) logarithmic slope and (4) maximal rotational velocity outside $2R_{25}/3$, (5) distance (Mpc, with $H_0 = 75 \text{ km s}^{-1} \text{ Mpc}^{-1}$), (6) ratio of inner fiducial radius $2R_{25}/3$ to fixed scale length distance $3b_{\text{opt}}$, and (7) source reference: Casertano & van Gorkom 1991 (CvG), or Broeils 1992 (B).

TABLE 2
DWARF GALAXY DATA

Name	$b_{\text{H I}}$ (kpc)	$M_{\text{lum}}/M_{\text{tot}}$	$R_{\text{out}}/b_{\text{H I}}$
DDO 154 ^a	1.65	0.11 ^b	4.6
NGC 2366 ^c	1.9 ^d	0.4 ^e	3.9
DDO 168 ^f	1.02	0.11	3.3
NGC 3109 ^g	3.5 ^d	0.08	2.3
DDO 170 ^h	3.1 ^d	0.08	4.1
NGC 1560 ⁱ	2.7 ^{d,i}	0.18	3.1

NOTES.—Columns list (1) name, (2) H I exponential scale length, (3) luminous-to-total mass ratio at the radial distance of the outermost velocity measurement, (4) Radial distance of the outermost velocity measurement in units of the H I scale length. Luminous mass include gas (H + He) and stars.

^a Carignan & Beaulieu 1989.

^b We have multiplied H I mass by 1.3 to take He into account.

^c Wevers 1984.

^d Our eye fit to the data.

^e We have added the gas mass to the quoted disk mass.

^f Broeils 1992.

^g Jobin & Carignan 1990.

^h Lake et al. 1990.

ⁱ Fit misses “bump” in surface density profile at $\approx 2b_{\text{H I}}$.

3109) mass models of the rotation curve suggest a subdominant stellar component (Jobin & Carignan 1990).

For the galaxies with $v_{\text{max}} > 80 \text{ km s}^{-1}$ we plot the logslope for $r \geq 3b_{\text{opt}}$. These latter points are all the same as the corresponding points in Figure 6a, except for the open symbols which represent galaxies whose slopes have changed by more than 0.05 when calculated from $3b_{\text{opt}}$ rather than $\frac{2}{3}$ of the optical radius. We have verified that the objects with $v_{\text{max}} \approx 90 \text{ km s}^{-1}$ (NGC 55, NGC 300, NGC 4236, and UGC 2259) have low gas mass-to-blue-light ratios $\lesssim 0.5$, or comparable optical and H I scale lengths (NGC 5585). Therefore we assume for these objects that the scale length of the baryonic mass distribution is the optical scale length.

In Figure 6c we overlay on the data of Figure 6b the logarithmic slopes as a function of the maximal velocity v_{max} of model rotation curves for disks of fixed mass corresponding to $v(R) = 50, 100, 200 \text{ km s}^{-1}$. This theoretical logarithmic slope is defined as the slope of a 21-point, straight-line least-squares fit to the log-log rotation curve with equally spaced radial distances. The logslopes are calculated in the radial distance range $r = 2-5b$ on the left side of the figure and for $3-8b$ on

the right side, corresponding to the data. The theoretical log-slopes are plotted for the expected range of halo λ 's, from 0.02 to 0.1. The reason these curves bend at logslope = 0 is that for falling rotation curves the maximum velocity is at some inner radius, while for rising rotation curves the maximum velocity is at the outer radius considered.

The data for all galaxies in Figure 6b appear to us consistent with the model predictions for a constant $F = 0.05$. The range of slopes shows at most a modest dependence on v_{\max} . We assume that the low number of small galaxies with negative slope might be due to the sparsity of the data, or possibly to a selection effect. Not surprisingly, there are many more data points for $\geq 200 \text{ km s}^{-1}$, for which it seems clearer that no trend of decreasing slope is present.

Small galaxies to the left of the vertical line show slopes that are compatible with the expectation for $F = 0.05$, although there is perhaps a better fit with $F = 0.025$ for all but the small galaxy with a negative slope (NGC 7793). (We note that the rotation curve of NGC 7793 has been analyzed taking warping into account [Carignan & Puche 1990]; forcing a flat outer rotation curve implies a much smaller inclination than is compatible with the outer optical and radio isophotes.) However the ratio of dark to luminous mass of the model galaxies inside, say, $4.5b_{\text{HI}}$ (see Fig. 4) is about a factor of 2–3 smaller than that indicated by the H I data (see Table 2). This could be evidence of gas loss. For small galaxies one would expect gas loss to be significant (cf. Dekel & Silk 1986), which would result in a small effective value of F in the adiabatic approximation.

Another feature of Figure 6 worth pointing out here concerns the range of values of v_{\max} for galaxies of fixed mass. If the range of values were too large, too much scatter would be introduced in the Tully-Fisher relation (note that for galaxies with negative slope the circular velocity reaches v_{\max} in the inner part of the galaxy). In fact, for $F = 0.05$ from Figure 6 we estimate a scatter of $\approx \pm 0.5 \text{ mag}$ for λ in the range 0.02–0.1 by simply estimating the range of values of v_{\max}^4 and neglecting the fact that the values of λ are not equally probable. We also find the scatter to be quite insensitive to changes in r_{core}/R , as long as it is not too small. It can be seen in the figure that for higher values of F the relative spread of values of v_{\max} increases. Thus, a rough estimate is that the scatter in the Tully-Fisher relation constrains $F \lesssim 0.05$.

To summarize our discussion thus far, we have considered the first correlation claimed by Casertano & von Gorkom (1991), between logarithmic slope and v_{\max} , and found that this trend almost disappears when consistent baryonic disk scale lengths are used throughout. When all the available data on both large and small galaxies are properly compared with our model, the data are consistent with the model prediction that there should not be a systematic relationship between logslope and v_{\max} except possibly for the galaxies with the smallest v_{\max} .

The second correlation discussed by Casertano & van Gorkom (1991, their Fig. 7) is that of logarithmic slope with disk scale length b . They find that bright galaxies ($v_{\max} > 180 \text{ km s}^{-1}$) with larger b have larger (more positive) slopes. From Figures 6 and 1 above, it is clear that such a correlation would be expected in our model as a result of the dispersion in protogalactic angular momentum λ . However, in order to study this correlation quantitatively the physics of the truncation radius R becomes crucial (in this model, at least, although perhaps not in real galaxies, which may form mainly by merging of subcondensations). If the gas in spiral galaxies has cooled quasi-statically inside their dark halos, then the gas collected

during the age of the universe has come from $R \approx 100(F/0.1)^{1/2} h^{-1/2} (v_c/300 \text{ km s}^{-1})^{1/2} \text{ kpc}$, as discussed above. Since $b \sim \lambda R$ for $\lambda = 0.02\text{--}0.1$ (see Fig. 1), this would imply $b \propto \lambda v_c^{1/2}$. Therefore, galaxies of constant luminosity would form sequences of increasing slope as a function of scale length, with brighter galaxies systematically shifted to larger scale lengths.

We have binned the data for large spirals in Casertano & van Gorkom (1991) in two bins in maximum velocity [$100 < (v_{\max}/\text{km s}^{-1}) < 200$, and $200 < (v_{\max}/\text{km s}^{-1}) < 300$] and find that indeed such a trend is clearly visible. At a given slope, however, the range of disk sizes predicted by the scaling $b \sim v_c^{1/2}$ is far too small. The inadequate range of disk sizes if $R \sim v_c^{1/2}$ is not surprising, because the total luminosity, $L_* \propto FM_{\text{total}} \propto F v_c^2 R$, should scale as v_c^4 . This would indicate that $R \sim v_c^2$ is needed. Such a scaling indeed provides a very good fit to the data.

It is worth noting that an alternative approach to solve the luminosity scaling problem proposed by White (1991) and White & Frenk (1991) instead invokes very efficient gas heating by star formation to keep a substantial fraction of the gas within R from cooling and falling in. The result is that the mass fraction of gas converted to stars is predicted to be $F_* \propto (v_c/300 \text{ km s}^{-1})^2 F$. This gives the correct Tully-Fisher scaling for the luminosity if R is independent of velocity (White 1991). However, from Figure 1b one can see that $b/R \sim F^{-1/3}$ at fixed λ . This implies $b \propto v_c^{-2/3}$ and, therefore, that brighter galaxies are predicted to have systematically smaller disks on average, which is opposite the trend in the data discussed by Casertano and van Gorkom.

4. CONCLUSIONS

We have investigated the systematic variations expected of spiral rotation curves if galaxies form from gas clouds that cool and radially collapse within dark matter halos. We have shown that several systematic trends seen in the data can be naturally explained as being due to variations in the angular momentum of protogalaxies with a universal gas-to-dark matter ratio $F \approx \langle \lambda \rangle$. In particular, the variation in protogalactic angular momentum expected in the tidal torque theory results in systematic variations in slope of the rotation curves to a degree that spans the range of variability seen in the data. Furthermore, if F is a universal constant, which is expected theoretically since the entropy per baryon is generated by microphysics that is not position-dependent, the value of F required, $F \approx \langle \lambda \rangle \approx 0.05$, agrees with nucleosynthesis constraints if the universe has a critical density of matter, and $H_0 \approx 50 \text{ km s}^{-1} \text{ Mpc}^{-1}$. With the data presently available, however, our calculations cannot exclude the possibility that protogalaxies have varying gas fractions. Additional data should shed light on this question, and perhaps uncover a clear break in the gas fraction of galaxies at the low-luminosity end.

A key ingredient in understanding the data quantitatively has been the halo compression due to baryonic infall, as demonstrated by the poor agreement with the data of the “stiff halo” curves in Figure 6c (comparing the range of logslopes in the data to the entire predicted range corresponding to $\lambda \approx 0.02\text{--}0.1$ expected from simulations). The detailed comparison with the data also points out the limitations of our model. Clearly the physics of the truncation radius R must be understood in order to further our understanding of the data. It is clear though that the quasi-static cooling of smooth gas clouds cannot explain the range of disk sizes and luminosities

of spiral galaxies. Since there is no reason to suppose that this would be a good approximation to the actual radial collapse of galaxies, it is perhaps encouraging that *both* disk sizes and luminosities require the same range of truncation radii, whereas conflicting variations would be required to explain them in terms of a variable gas fraction F . In fact, if substantial subclustering existed in protogalaxies, as expected in cold dark matter models, it might have led to a very lumpy radial collapse. Also, while most of the trends we have discussed are not very sensitive to the value of the core radius of protogalaxies before infall, they do require the core radius to be sufficiently large. The exact mechanism by which this would happen remains to be uncovered, and it is not clear to us whether the most recent large-scale simulations (Dubinski & Carlberg 1991; Warren et al. 1992) definitely rule out the possibility of

large core radii for cold dark matter halos. If high-resolution dissipationless cold dark matter simulations really do give small core radii, perhaps the dark matter is of a different sort, or perhaps transfer of angular momentum from dissipative baryonic material to the dissipationless halo inhibits its collapse at the core (Katz & Gunn 1991; N. Katz 1992, private communication).

Our work has been supported by NSF, CalSpace, and Faculty Research grants at UCSC, and by a Research Fellowship at the University of Missouri-St. Louis. The work of R. F. has also been partly funded by Fundación Andes. We thank Stephane Courteau, John Kormendy, Lars Hernquist, and Jacqueline von Gorkom for helpful conversations.

REFERENCES

- Amram, P., et al. 1993, *ApJ*, 403, L59
 Athanassoula, E., Bosma, A., & Papaioannu, S. 1987, *A&A*, 179, 23
 Bahcall, J. N., & Casertano, S. 1985, *ApJ*, 293, L7
 Barnes, J. 1987, in *Nearly Normal Galaxies*, ed. S. Faber (NY: Springer), 154
 Barnes, J., & Efstathiou, G. 1987, *ApJ*, 319, 575
 Blumenthal, G. R. 1988, in *IAU Symp. 130, Large-Scale Structures in the Universe*, ed. J. Audouze, M. Pelletan, & A. Szalay (Dordrecht: Kluwer), 421
 Blumenthal, G. R., Faber, S. M., Flores, R., & Primack, J. P. 1986, *ApJ*, 301, 27 (BFPP)
 Blumenthal, G. R., Faber, S. M., Primack, J. P., & Rees, M. J. 1984, *Nature*, 311, 527 (BFPR)
 Broeils, A. 1992, Ph.D. thesis, Univ. Groningen
 Burstein, D., & Rubin, V. C. 1985, *ApJ*, 297, 423
 Carignan, C., & Freeman, K. C. 1988, *ApJ*, 332, L33
 Carignan, C., & Puche, D. 1990, *AJ*, 100, 394
 Casertano, S., & van Gorkom, J. H. 1991, *AJ*, 101, 1231
 Chandrasekhar, S. 1960, *Principles of Stellar Dynamics* (NY: Dover)
 Dekel, A., Bertschinger, E., Yahil, A., Strauss, M. A., Davis, M., & Huchra, J. P. 1993, *ApJ*, 412, 1
 Dekel, A., & Silk, J. 1986, *ApJ*, 303, 39
 Dubinski, J., & Carlberg, R. G. 1991, *ApJ*, 378, 496
 Efstathiou, G., & Jones, B. J. T. 1979, *MNRAS*, 186, 133
 Fall, S. M., & Efstathiou, G. 1980, *MNRAS*, 193, 189
 Flores, R. 1987, in *Cosmology and Particle Physics*, ed. I. Hinchliffe (Singapore: World Scientific), 48
 Flores, R., Blumenthal, G. R., Dekel, A., & Primack, J. R. 1986, *Nature*, 323, 781
 Flores, R. A., & Primack, J. R. 1993, Santa Cruz preprint SCIPP 93/91
 Freeman, K. 1970, *ApJ*, 160, 811
 Frenk, C. S., et al. 1985, *Nature*, 317, 595
 Gilmore, G. F., King, I., & van der Kruit, P. C. 1990, *The Milky Way as a Galaxy* (Mill Valley, CA: University Science Books)
 Hernquist, L. 1990, *ApJ*, 356, 369
 Hoyle, F. 1949, *Problems of Cosmological Aerodynamics*, ed. J. M. Burges & H. C. van Hulst (Paris: IAU), 195
 Jobin, M., & Carignan, C. 1990, *AJ*, 100, 648
 Katz, N. 1992, *ApJ*, 391, 502
 Katz, N., & Gunn, J. E. 1991, *ApJ*, 377, 465
 Kent, S. 1985, *ApJS*, 59, 115
 ———. 1986, *AJ*, 91, 1301
 ———. 1987, *AJ*, 93, 816
 Lake, G., Schommer, R. A., & van Gorkom, J. H. 1990, *AJ*, 99, 547
 Lynden-Bell, D. 1967, *MNRAS*, 136, 101
 Nusser, A., & Dekel, A. 1993, *ApJ*, 405, 437
 Oh, K. S. 1990, Ph.D. thesis, Univ. California-Santa Cruz
 Olive, K. A., Schramm, D. N., Steigman, G., & Walker, T. P. 1990, *Phys. Lett. B*, 223, 454
 Peebles, P. J. E. 1969, *ApJ*, 155, 393
 Persic, M., & Salucci, P. 1991, *ApJ*, 368, 60
 Persic, M., Ashman, K. M., & Salucci, P. 1991, *ApJ*, 379, 89
 Quinn, P. J., Salmon, J. K., & Zurek, W. H. 1986, *Nature*, 322, 329
 Rees, M. J., & Ostriker, J. P. 1977, *MNRAS*, 179, 541
 Ryden, B. 1988, *ApJ*, 329, 589
 Ryden, B., & Gunn, J. E. 1987, *ApJ*, 318, 15
 Shu, F. H. 1978, *ApJ*, 225, 83
 Simien, F., & de Vaucouleurs, G. 1986, *ApJ*, 302, 564
 Smoot, G. F., et al. 1992, *ApJ*, 396, L1
 Steigman, G., Sarazin, C. L., Quintana, H., & Faulkner, J. 1978, *AJ*, 83, 1050
 van Albada, T. S., Bahcall, J. N., Begeman, K., & Sancisi, R. 1985, *ApJ*, 295, 305
 van Albada, T. S., & Sancisi, R. 1986, *Phil. Trans. R. Soc. Lond.*, A2330, 447
 van der Kruit, P. A. 1990, in *IAU Symp. 139, Galactic and Extragalactic Background Radiation: Optical, Ultraviolet, and Infrared Components* ed. S. Bowyer & C. Leinert (Dordrecht: Kluwer), 85
 Walker, T. P., Steigman, G., Schramm, D. N., Olive, K. A., & Kang, H.-S. 1991, *ApJ*, 376, 51
 Warren, M. S., Quinn, P. J., Salmon, J. K., & Zurek, W. H. 1992, *ApJ*, 399, 405
 White, S. D. M. 1991, in *IAU Symp. 146, The Dynamics of Galaxies and the Molecular Cloud Distribution*, ed. F. Combes & F. Casoli (Dordrecht: Kluwer), 383
 White, S. D. M., & Frenk, C. 1991, *ApJ*, 379, 52
 White, S. D. M., & Rees, M. J. 1978, *MNRAS*, 183, 341
 Whitmore, B. C., Forbes, D. A., & Rubin, V. C. 1988, *ApJ*, 333, 542
 Zel'dovich, Ya. B., Klypin, A. A., Khlopov, M. Yu., & Chechetkin, V. M. 1980, *Soviet J. Nucl. Phys.*, 31, 664